Energy Exchange Dynamics across L-H transitions in NSTX

A. Diallo[1*], S. Banerjee[2], S. Zweben[1], and T. Stoltzfus-Dueck[1]
[1] Princeton Plasma Physics Laboratory, Princeton, NJ, USA.
[2]Institute for Plasma Research, Bhat, Gandhinagar 382428, Gujarat, India.
*E-mail address of main author: adiallo@pppl.gov

Understanding the trigger mechanism that leads to the transition between the low (L) and high (H)-confinement plasma in tokamak devices remains one of the most outstanding theoretical and experimental challenges for fusion science, and it is critical for ITER operation. The motivation is to rigorously test the L-H transition models (e.g., predator-prey and ExB flow suppression), while also exploring other possible explanations, we investigate the energy exchange dynamics across L-H transitions using the gas-puff imaging (GPI) for high temporal and spatial resolution on NSTX.

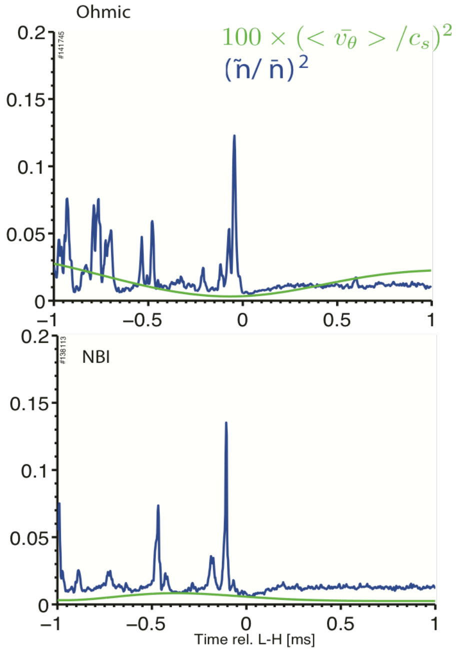

Figure 1: Comparison of the electron thermal free energy and kinetic energy due to the mean flow across the L-H transitions. Top panel represents an example of an Ohmic discharge. The bottom panel is that of an NBI discharge. In both cases, the thermal free energy is much larger than the kinetic energy in the mean flows.

In our analysis, we use a novel orthogonal decomposition programming (ODP) approach[1] to infer both the radial and poloidal velocities across the L-H transition in all types of discharges (e.g., Ohmic, RF, and NBI). The inferred velocities are decomposed into mean and fluctuating components. The latter component is represented by frequencies greater than 500 Hz. The mean poloidal flow at 1 cm inside the last-closed flux surface (LCFS) does not systematically increase over the 1 ms observation window across the L-H transition. Similar lack of systematic increase across the L-H transition of the flows was reported for DIII-D [2].

In the predator-prey model, energy is depleted from turbulent/fluctuating ExB velocities via transfer to mean flows. However, rapid electron parallel conduction strongly couples electron pressure fluctuations with the fluctuating/nonzonal ExB flows, and will replenish the energy in those flows on the electron transit timescale. So, in order for transfer to mean flows energy ($0.5\mathrm{m_i}\langle\bar{\mathrm{v}}_\theta\rangle^2$) to suppress the turbulence, the energy transferred must be significant relative to not only fluctuating ExB kinetic energy ($0.5\mathrm{m_i}\langle\tilde{v}_\perp\rangle^2$) but also electron thermal free energy ($0.5\mathrm{T_e}\left[\tilde{\mathrm{n}}_\mathrm{e}/\bar{\mathrm{n}}_\mathrm{e0}\right]^2$) [3]. Figure 1 displays the kinetic energy in the mean poloidal flow along with the electron thermal free energy, both normalized to $0.5\mathrm{T_e}$, evaluated 1 cm inside the LCFS. (Here, the rms GPI intensity relative to the mean GPI intensity is used as proxy for $\tilde{n}_e/\bar{n}_{e0}$). In this figure, the free thermal energy is always much greater than the kinetic energy in the mean poloidal flow, which is inconsistent with the exchange energy paradigm of the predator-prey model.

Figure 2 displays the poloidally averaged (defined by the brackets < >) poloidal velocities, the Reynolds stress (as $\langle\tilde{v}_\theta\tilde{v}_r\rangle$), and the production term as $\langle\tilde{v}_\theta\tilde{v}_r\rangle\partial_r\langle\bar{v}_\theta\rangle$ across the L-H

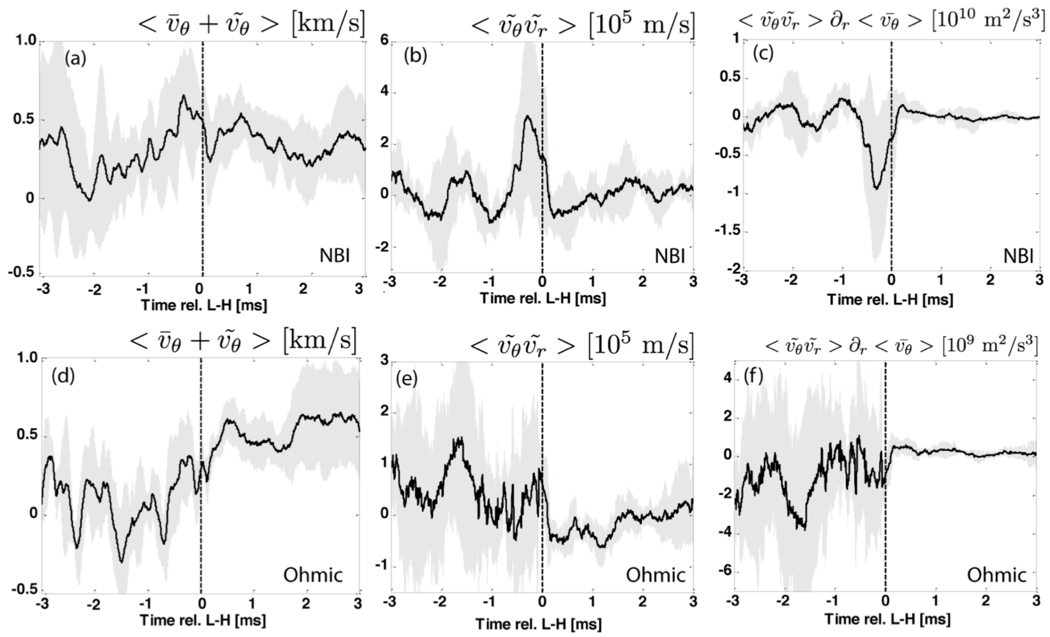

Figure 2: Time evolution, across the L-H transitions of NBI (top row) and Ohmic (bottom row) discharges. (a) & (d) display the poloidal velocities; (b) & (e) the Reynolds stresses; (c) & (f) the production terms. All these quantities are evaluated 1 cm inside the last-closed flux surface. The grey shaded area represents the root-mean-square deviations over multiple discharges at the same radial location (1 cm) relative to the LCFS.

transition in Ohmic and NBI discharges. All these quantities are localized 1 cm inside the LCFS. Prior to the L-H transition, there is no significant change of the poloidal flows as shown in figure 2 (a) & (c) approximately 1 cm inside the LCFS. Quantitavely similar trends of the temporal evolution of the poloidal flow evaluated at 2 cm inside the separatrix (no shown here) suggest minimal changes in shear rate across the L-H transitions. Figure 2 (b) & (e) displays the Reynolds stress, which remains positive with no consistent excursion prior the L-H transition. Finally, The production term, that represents energy exchange, is negative prior to the L-H transition, which suggests that the energy flows from DC flows to turbulence. This is again inconsistent with the transfer of energy from fluctuations to mean flow for turbulence suppression. These observations are at odds with the predator-prey model often proposed as a mechanism for the L-H transition.

In this paper, we report on the investigation of the L-H transition dynamics for three sets of 17 discharges (Ohmic, RF, and NBI) using an edge-localized turbulence imaging system, namely GPI. This system has a temporal resolution of 2.5 μs per frame and up to ~ 1 cm spatial resolution over 24 x 30 cm at the outer midplane edge. Based on this temporal and spatial resolution, a velocimetry analysis using the novel orthogonal ODP approach provides the edge 2D velocity field at high spatial and temporal resolution across the L-H transition. Detailed comparison between the ODP, the time-delay estimate, and the spatial correlation technique will be reported.

In summary, the results presented here are at odds with the predator prey model where the energy transfer from turbulence to DC flows is key in triggering the L-H transition. Furthermore, the results are inconsistent with the time sequence of the L-H transition and the positive production term (transfer from turbulence to DC flows) increasing before the L-H transition as highlighted in ref [4]. Additional studies of the radial correlation dynamics across the L-H transition will be reported. This work was performed under US DoE contract # DE-AC02-09CH11466 at PPPL. [1] Banerjee et. al., Rev. Sci. Instrum. 86, 033505 (2015); [2] McKee et al Nucl. Fusion 49 115016 (2009); [3] Scott, Phys. Plasmas, 12, 062314 (2005); [4] Cziegler et al., Plasma Phys. Control. Fusion 56 075013 (2014);